Applied Microscopy
Korean Society of Microscopy

pISSN 2287-5123 · eISSN 2287-4445
http://dx.doi.org/10.9729/AM.2016.46.1.6

Regular Article

Real-time Fluorescence Lifetime Imaging Microscopy Implementation by Analog Mean-Delay Method through Parallel Data Processing

Jayul Kim, Jiheun Ryu, Daegab Gweon*

Department of Mechanical Engineering, Korea Advanced Institute of Science and Technology (KAIST), Daejeon 34141, Korea

*Correspondence to:
Gweon D,
Tel: +82-42-350-3225
Fax: +82-42-350-5225
E-mail: gweondg@kaist.ac.kr

Received January 5, 2016
Revised February 29, 2016
Accepted March 2, 2016

Fluorescence lifetime imaging microscopy (FLIM) has been considered an effective technique to investigate chemical properties of the specimens, especially of biological samples. Despite of this advantageous trait, researchers in this field have had difficulties applying FLIM to their systems because acquiring an image using FLIM consumes too much time. Although analog mean-delay (AMD) method was introduced to enhance the imaging speed of commonly used FLIM based on time-correlated single photon counting (TCSPC), a real-time image reconstruction using AMD method has not been implemented due to its data processing obstacles. In this paper, we introduce a real-time image restoration of AMD-FLIM through fast parallel data processing by using Threading Building Blocks (TBB; Intel) and octa-core processor (i7-5960x; Intel). Frame rate of 3.8 frames per second was achieved in 1,024×1,024 resolution with over 4 million lifetime determinations per second and measurement error within 10%. This image acquisition speed is 184 times faster than that of single-channel TCSPC and 9.2 times faster than that of 8-channel TCSPC (state-of-art photon counting rate of 80 million counts per second) with the same lifetime accuracy of 10% and the same pixel resolution.

Key Words: Analog mean-delay fluorescence lifetime imaging microscopy, Parallel processing, Fluorescence lifetime, Confocal microscopy, Real time

INTRODUCTION

Fluorescence lifetime imaging microscopy (FLIM), especially based on the most accurate and frequently used technique called time-correlated single photon counting (TCSPC), has been widely employed for it gives not only morphological information but also chemical information. Chemical properties such as pH value (Hanson et al., 2002), ion or oxygen concentration (Gilbert et al., 2007), molecular dynamics and even the disease progression (Park et al., 2012) can be investigated and studied by TCSPC-FLIM. This powerful traits of FLIM has led many researchers and developers to include FLIM into their imaging system.

Even though TCSPC-FLIM technique gives precise and accurate measurement of fluorescence decay curves, its core technology, called single photon counting (SPC), inherently limits the system from high speed imaging. In the case of the state-of-art single channel TCSPC-FLIM, more than one minute is required to produce an image of 512 by 512 pixels with 10% accuracy. The acquisition time could be lengthened up to five minutes for 3% accuracy (Köllner & Wolfrum, 1992).

To overcome such drawback of the long acquisition time of TCSPC-FLIM, analog mean-delay FLIM (AMD-FLIM) was recently developed (Moon et al., 2009; Won et al., 2009). Rather than using the stochastic reconstruction used in SPC techniques, AMD method extracts a decay constant directly by subtracting the mean-delay time (or mean-arrival time) of reflected photon flux from that of fluorescence photon flux. The total amount of alterations in the mean-delay time

caused by the instrument characteristics are exactly the same between fluorescence photon flux and reflected photon flux, if they share the beam path and optical components. Then, the difference between those two mean-delay times would converge to the fluorescence lifetime.

The mean-delay time of photon flux is measured from the temporal distribution of photon flux. For it represents the result of successive convolutions of all factors causing temporal broadening or temporal delay (e.g., laser pulse width, optical path length, fluorescence lifetime, detector time-spread and electronic bandwidth), the distribution used in AMD method is different from the stochastically reconstructed histogram of TCSPC method. Moreover, in contrast to the TCSPC method, AMD-FLIM encourages such temporal distributions to be broadened for the convenience of measurements. Temporal distribution curves of fluorescence and reflected photon flux is shown in Fig. 1. The term IRF denotes an impulse response function (IRF) in AMD-FLIM, for the back scattering process on a reflective surface can be regarded as an impulse compared to the fluorescence process. Measuring IRF is essential because it carries all instrumental information needed to extract only the fluorescence lifetime from the fluorescence distribution curve.

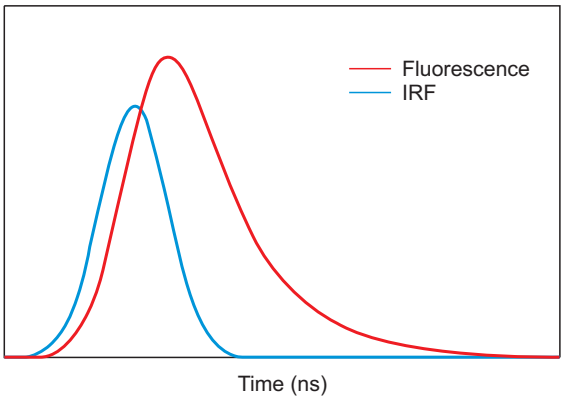

Fig. 1. Impulse response function (IRF) and fluorescence signal.

The fluorescence lifetime can be calculated by subtracting the mean-delay time (the first moment of the temporal distribution curve) of IRF from that of fluorescence as shown in equation (1) below.

$$\tau = \langle T_e \rangle - \langle T_e^0 \rangle = \frac{\int t \cdot i_e(t)dt}{\int i_e(t)dt} - \frac{\int t \cdot i_{irf}(t)dt}{\int i_{irf}(t)dt} \quad (1)$$

$i_{irf}(t)$ is an IRF signal measured without a fluorescence emission filter and bracketed (which means time-averaged) blue $<T_e^0>$ is the mean-delay time of IRF signal. Meanwhile, $i_e(t)$ is a fluorescence signal measured with a fluorescence emission filter and bracketed red $<T_e>$ is the lifetime broadened as much as the lifetime of a fluorophore.

Although AMD-FLIM opened a way to real-time FLIM, previous researchers could not implement the system on real time basis. That is mainly because it is not an easy task to process a great load of data and to make frames on real time basis. In this paper, those obstacles are to be addressed and as a result, fluorescence lifetime imaging with a frame rate of 3.8 frames/sec is achieved in 1,024×1,024 pixel resolution. This frame rate is limited mechanically by the speed of 4-kHz resonant scanner utilized in the experiment, but not by data processing speed.

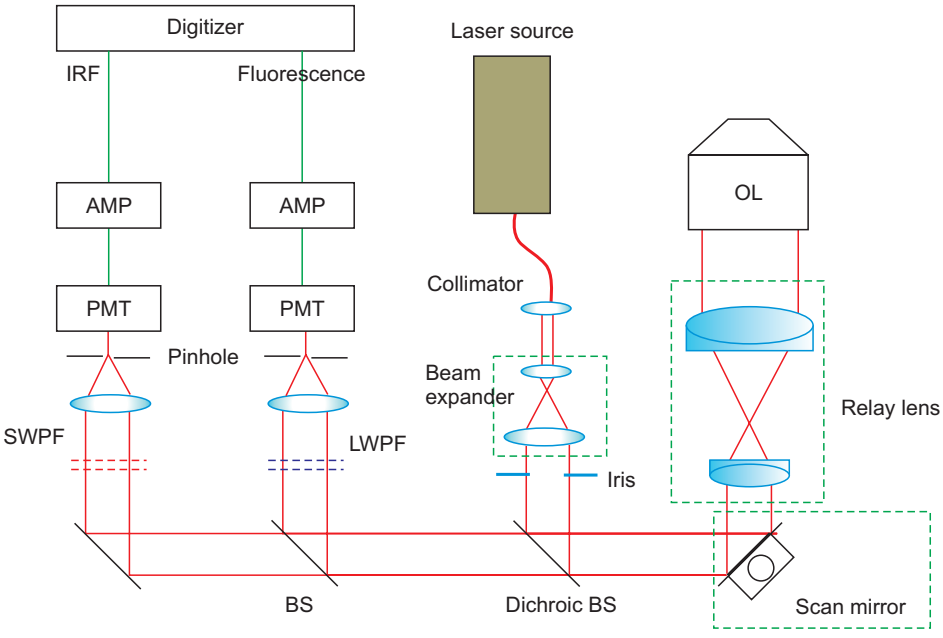

Fig. 2. Schematic diagram of analog mean-delay fluorescence lifetime imaging microscopy setup. IRF, impulse response function; AMP, amplifier; PMT, photomultiplier tube; SWPF, short wavelength pass filter; LWPF, long wavelength pass filter; BS, beam-splitter; OL, objective lens.

In the previous researches, single photomultiplier tube was used so that the mean-delays of IRF and fluorescence were measured by removing and inserting a fluorescence emission filter respectively (Moon et al., 2009). The optical path difference by the existence of the filter could be neglected but a trigger time difference caused considerable errors in the result (Won et al., 2010). In this paper, however, IRF and fluorescence lifetimes are collected and triggered simultaneously along two separate photomultiplier tubes, so that the redundant compensation is unnecessary.

MATERIALS AND METHODS

The schematic diagram of the system is shown in Fig. 2. A picosecond pulsed laser (PicoTA 780; PicoQuant and Toptica Photonics, Germany) of which the wavelength is 780 nm was utilized. The pulse repetition rate can be changed among 40 MHz, 20 MHz, 10 MHz, 5 MHz, 2.5 MHz internally and any number of Hz between those values if externally triggered. Pulse width is 100 ps full width at half maximum. Single mode fiber patch cable was connected between the laser and a collimator of 18 mm focal length. Laser beam power was measured as 2 mW after the beam is collimated. A Galilean beam expander (BE03M-B-3X; Thorlabs, USA) was set before two-axis scan mirrors (CRS-4k and 6230H; Cambridge Technology, UK) to fill effective clear aperture of them. A double-telecentric relay optics, which is composed of two achromatic doublets (scan lens with 160 mm effective focal length) and one achromatic doublet (tube lens with 400 mm focal length), were designed to acquire low aberration images. Long-pass emission filter (FF01-832/37; Semrock, USA) and short-pass emission filter (FF01-769/41; Semrock) were placed along the beampaths of fluorescence and IRF channels respectively. Focusing lenses (singlet, 150 mm focal length) and pinholes (50 μm diameter) were set between the emission filter and a photomultiplier tube (PMT) of each beampath to build a confocal-FLIM microscope.

Two PMTs (H7826-01; Hamamatsu Photonics, Japan) were used to detect fluorescence and IRF signals. The PMTs are current output type and its maximum output current is 100 μA. High-bandwidth amplifiers (C9663; Hamamatsu Photonics) were used to convert current signal outputs of the PMTs into voltage signals (conversion ratio is 4 mV/μA and 3 dB bandwidth is 150 MHz). This combination of H7826-01 and C9663 provides maximum 400 mV output signal to analog to digital (A/D) converter.

A two-channel high-speed digitizer (U5309A; Keysight Technologies, USA) with low voltage and triggered simultaneous acquisition and readout (TSR) option was utilized for A/D converting. Its sampling rate is 1 GS/s and its bandwidth is 300 MHz at 3 dB. Minimum input voltage range is 50 mV and the maximum is 1 V. With TSR option, one data set can be fetched into local personal computer (PC)'s random access memory (RAM) while other data set is acquired into digitizer's RAM. Sampling rate of 1 GS/s is sufficient for signals with 1.4 ns or more half width half maximum (HWHM) (Kim et al., 2015). Faster sampling than 1 GS/s prevents real time data fetching from an A/D converter to PC RAM, which inevitably leads to a failing of real time implementation of the whole system.

Both amplifiers and a digitizer were selected to have a

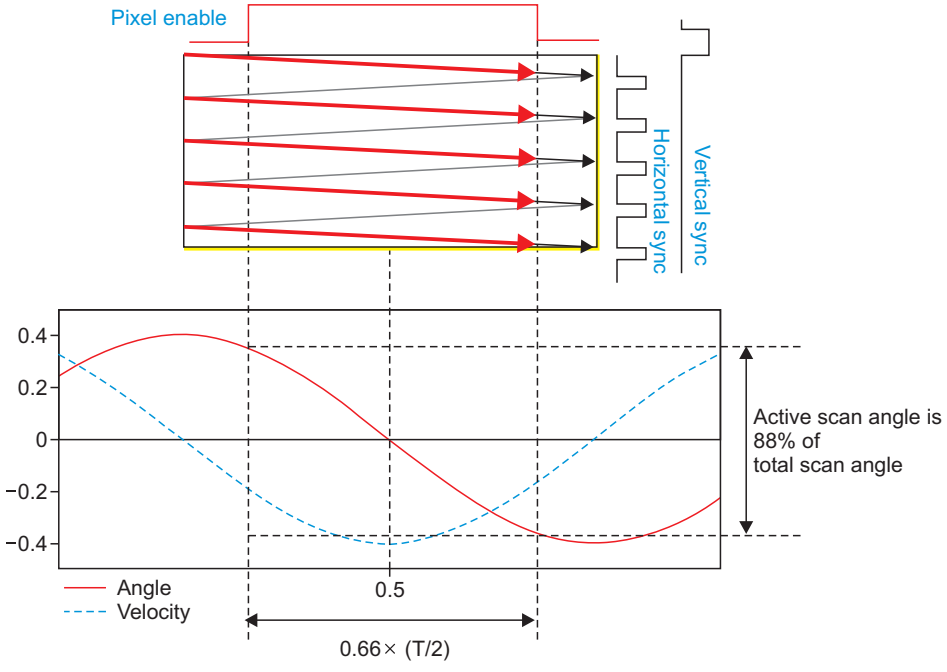

Fig. 3. Three synchronization signals utilized in the system are represented in the above. Below is the angular position and velocity profiles of a 4-kHz resonant scanner. Revised from CRS (Counter Rotation Scanner) User's Manual (Cambridge Technology, 2006). T=scanner oscillation period.

function to adjust the input offset, which plays a crucial part to eliminate background noises.

Frame Composition and Triggering Circuit

To visualize the two-dimensional lifetime distribution in the region of interest of the specimen, it is required to constitute frames using three synchronization signals; horizontal sync (line sync) signal, vertical sync (frame sync) signal, and 'pixel enable' signal. Three synchronization signals are represented in Fig. 3 (Cambridge Technology, 2006). To construct two dimensional laser scanning microscopy, a 4-kHz resonant scanner and a 1-kHz galvanometer scanner were utilized for fast-axis (horizontal) and slow-axis (vertical) scanning respectively. Horizontal sync signals should be generated at each round-trip end of the resonant scanner to distinguish the lines. Vertical sync signals are generated by an analog input-output board (PCI-6733; National Instruments, USA) to distinguish the frames. Each vertical sync is generated after all horizontal lines for a frame are counted.

Control electronics of the resonant scanner provides 'pixel enable' signals to mark the active scan range, namely, relatively constant velocity range, which occupies the 66 percent of half the period (when uni-directionally scanned) of the resonant scanner. Trigger signals for a digitizer are created from the composition of 'laser pulse clock', 'pixel enable' and 'vertical sync', of which the procedure is described in Fig. 4. D flip-flop was used to synchronize the start of a trigger with the first detected rising edge of a 'laser pulse clock' when 'pixel enable' signal turns high. Effective 'pixel enable' signals are discriminated by a vertical sync signal via AND gate and NOT gate. Configuration of an electric circuit for the generation of triggering signals is well represented in Fig. 5. A line-receiver is used to convert differential signals to transistor to transistor logic (TTL) signals and line-driver is inserted to transform TTL signals back into differential signals.

Data Acquisition, Fetch and Processing on Real-Time Basis

Data from amplifiers are triggered line by line horizontally and sampled at 1 GS/s and collected into RAM of a digitizer, which process is called as acquisition. Thereafter, data are fetched to RAM of a PC and are subsequently processed. This procedure is displayed in Fig. 6. Acquisition and fetching must be performed almost con-currently not to miss the start of the next frame, which is effectively facilitated by TSR function of the digitizer. Processing the fetched data within the return time of a galvanometer scanner is nearly impossible. To overcome this problem, ring buffered frames were structured to ensure reliable data processing (Fig. 7). Frame numbers in ring buffer are locked with mutex after data are fetched and written to the specified buffer and unlocked after the data are processed.

Although a buffered frame structure was utilized, fetched data should be processed well within acquisition and fetch time not to be piled up. With 40 MHz pulse repetition rate equivalent to 25 ns pulse window size, for example, data processing time

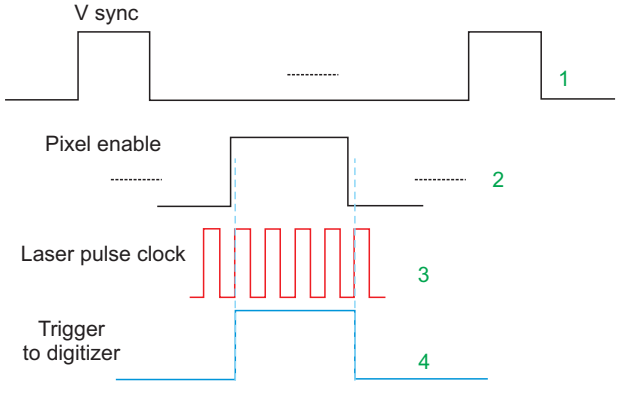

Fig. 4. How to configure trigger signals for a digitizer.

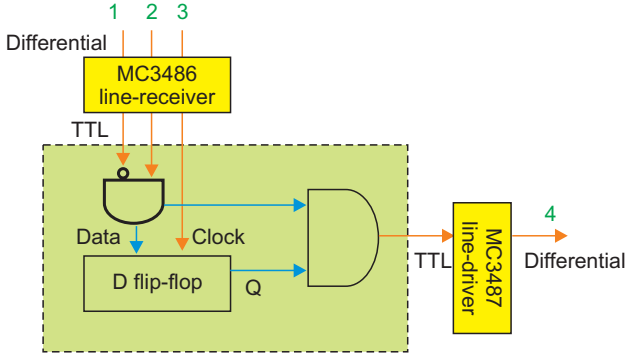

Fig. 5. Electric circuit to generate triggering signals. TTL, transistor to transistor logic.

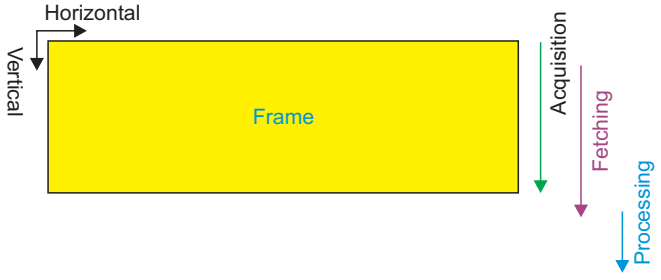

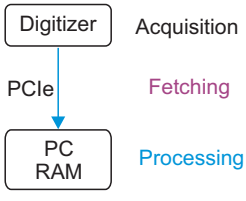

Fig. 6. Digitized data are acquired and fetched and processed consecutively. PCIe, peripheral compenent interconnect express; PC, personal computer; RAM, random access memory.

must be sufficiently lower than 25 ns, because a processor has to perform various tasks other than processing, such as fetching, image processing, storage, etc.

In this regard, parallel computing on real-time basis is compulsory. In Fig. 8, unit operation times with or without parallel processing are charted. Unit operation here is defined as processing the data from one laser pulse. All measurements were performed on visual studio 2013 release mode and averaged 1 giga times. Parallel processing was bench-tested with Open Multi-Processing (OpenMP; OpenMP Architecture Review Board) and Intel Threading Building Blocks (TBB; Intel, USA). With Intel TBB known as optimized for Intel core, 0.7 ns per unit operation could be accomplished. Octa core of i7-5960x with 20M cache and x99 chipset and 32G DDR4 RAM were employed.

In this structure, frames of 1,024×1,024 resolution could be processed into FLIM images with a frames rate of 3.8 frames/sec, which is equivalent to a pixel rate of 3.98 Mpixel/sec. Since AMD-FLIM is compatible with high power laser and a photon rate is sufficient compared to TCSPC-FLIM, the major limiting factor of imaging speed is not the photon rate but 2-dimensional scanning speed.

As far as TCSPC is concerned, the number of photons required to achieve 10% accuracy in one pixel is known to be higher than 185 (Köllner & Wolfrum, 1992). This means

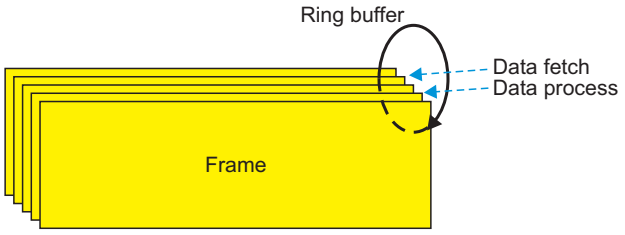

Fig. 7. Ring buffered frames for data to be fetched and processed reliably. Fetch thread is always followed by process thread to secure data credibility.

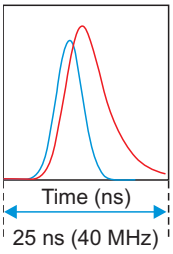

$$\tau = \langle T_e \rangle - \langle T_e^0 \rangle = \frac{\int t \cdot i_e(t)dt}{\int i_e(t)dt} - \frac{\int t \cdot i_{irf}(t)dt}{\int i_{irf}(t)dt}$$

@ Microsoft Visual Studio 2013
release mode 1 giga-times averaged

Processing method	Unit operation time (ns)	Type
x86	54	Single thread processing
x64	26	
OpenMP	3.6	Parallel processing (8 threads) @ x64 machine
TBB	0.7	

Only $i\varepsilon(t)$ is processed in this time measurement

Fig. 8. Unit operation time with or without parallel processing. TBB, Threading Building Blocks.

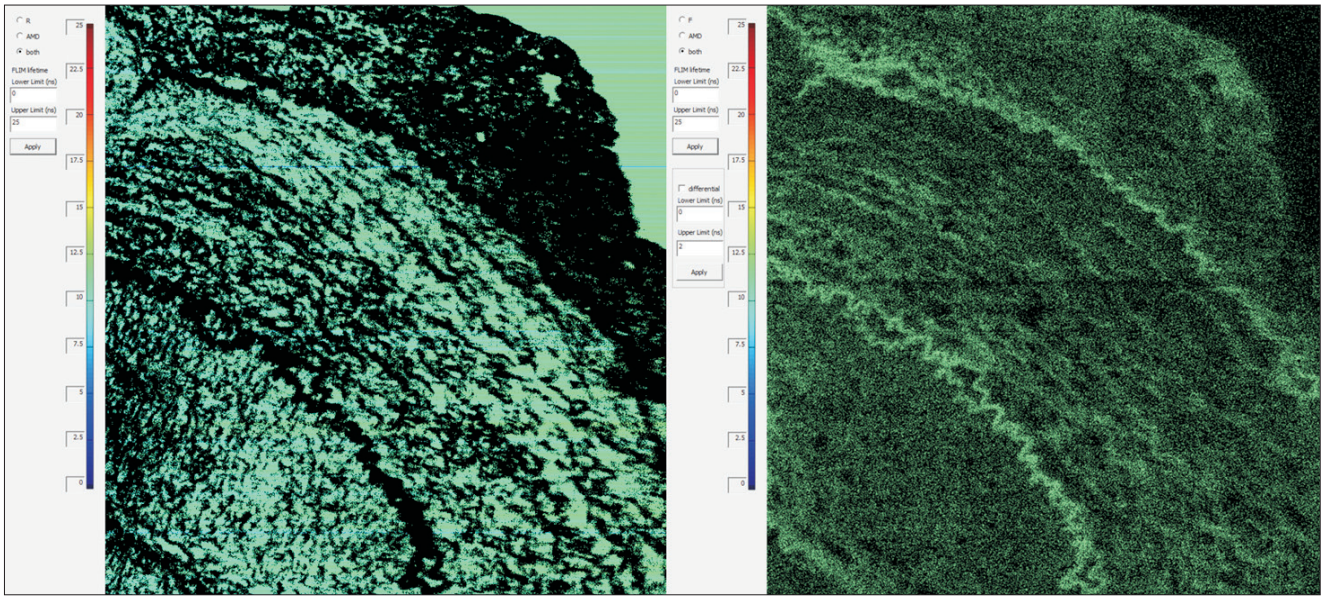

Fig. 9. Microsoft Foundation Class interface for lifetime images. Left is a lifetime image for impulse response function and right is for fluorescence.

that generating a single frame in 1,024×1,024 resolution by TCSPC takes 48.5 second, assuming that maximum photon rate is 4 Mcps to prevent 80-MHz pulsed laser from causing severe data distortion by pile-up effect. Therefore, the imaging speed of our AMD-FLIM system is 184 times faster than single-channel TCSPC and 9.2 times faster than state-of-art 8-channel TCSPC (assuming that each pile-up free channels has 10 Mcps photon counting rate) with 10% accuracy.

In addition to FLIM images, simple reflection and fluorescence images can be constructed at the same time, for the denominator in equation (1) implies that information. The user interface of Microsoft Foundation Class (MFC) for sample FLIM image is depicted in Fig. 9. The lifetimes are mapped into color by standard jet colormap.

RESULTS AND DISCUSSION

To evaluate the accuracy of AMD-FLIM, indocyanine green

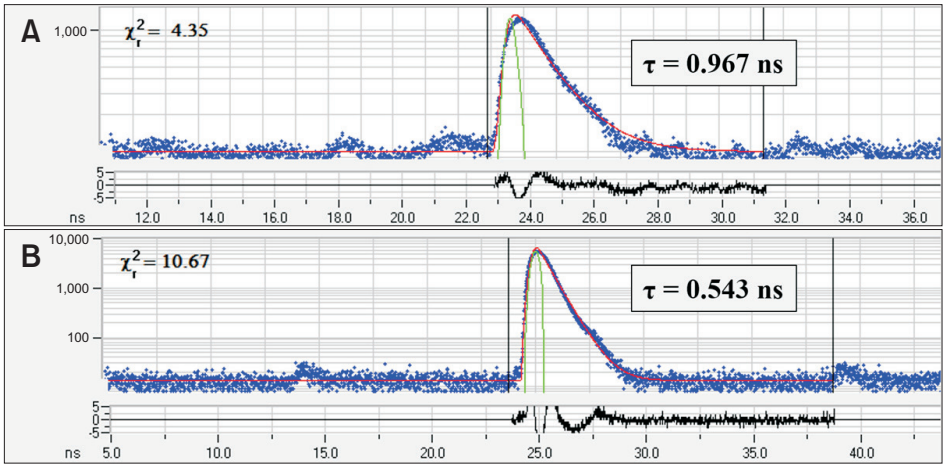

Fig. 10. Lifetime measurements by time-correlated single photon counting. (A) Indocyanine green (ICG) dissolved in dimethyl sulfoxide. (B) ICG dissolved in methanol.

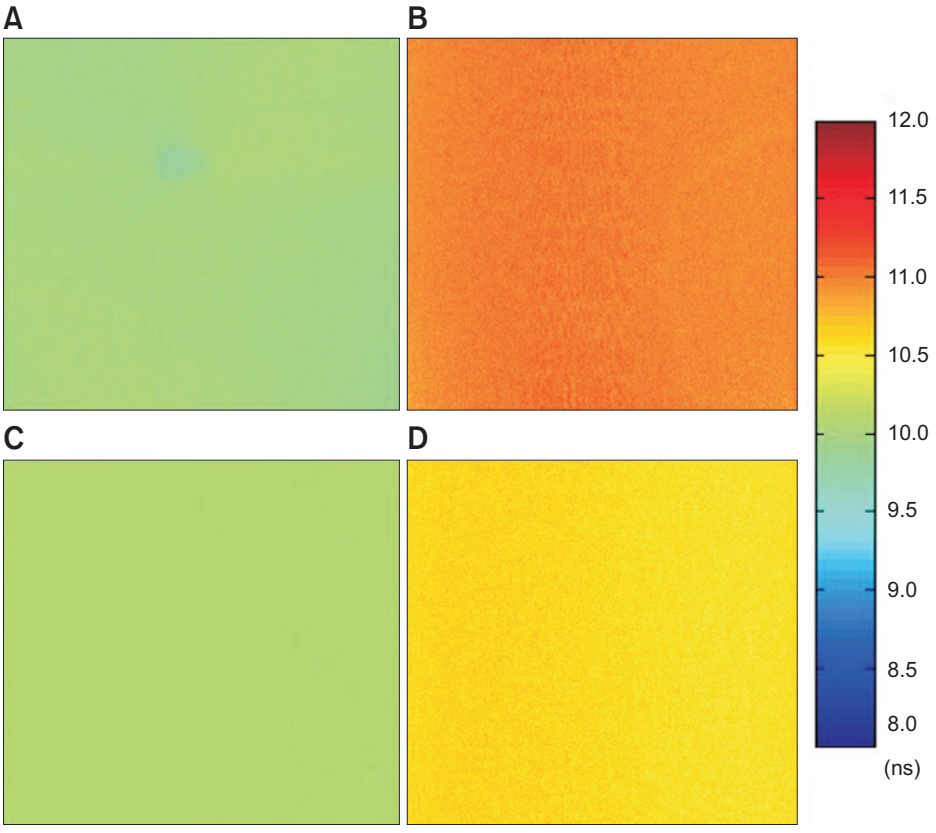

Fig. 11. Lifetime measurements by analog mean-delay. (A) Impulse response function (IRF) image from indocyanine green (ICG) dissolved in dimethyl sulfoxide (DMSO). (B) Fluorescence image from ICG dissolved in DMSO. (C) IRF image from ICG dissolved in methanol. (D) fluorescence image from ICG dissolved in methanol.

(ICG) as a fluorophore, and dimethyl sulfoxide (DMSO) and methanol as solvent were employed. Even though the lifetimes of ICG solutions made by such solvents are known as 0.97 ns and 0.51 ns respectively (Berezin & Achilefu, 2010), these values might be varied depending on several experiment conditions. Because all the factors might not be reproduced exactly as the reference (Berezin & Achilefu, 2010), TCSPC scheme, known as the most accurate scheme of the lifetime measurements, was implemented to obtain the real lifetime values. By replacing fluorescence channel detector with a photon-counting photomultiplier tube (H7422P-50; Hamamatsu Photonics), single-photon signals could be acquired without changing any other optical components. Then, a single-channel TCSPC module (SPC-150; Becker and Hickl GmbH, Germany) and detector control electronics (DCC-100; Becker and Hickl GmbH) were used to measure real lifetimes accurately.

The concentration of ICG solutions was controlled at around 10 μM. The reference lifetime data obtained by TCSPC scheme is shown in Fig. 10. Measured lifetime is 0.97 ns and 0.54 ns when ICG is dissolved into DMSO solvent and methanol solvent respectively. TCSPC measurements were performed by using SPCM software (v.9.30; Becker and Hickl GmbH) and were analyzed by using SPC Image software (v.3.2.3; Becker and Hickl GmbH). The lifetime distribution of the solutions, which is expected to be uniform, is acquired by our confocal AMD-FLIM configuration and shown in Fig. 11. The lifetime was calculated by subtracting mean delay value of IRF channel from that of fluorescence channel. In the case of the dye dissolved in DMSO, 1.05 ns with standard deviation of 0.12 ns was measured and the error was 8.3% compared with the result given by TCSPC. The standard deviation was evaluated by average values of 20 successive measurements. When in methanol, 0.58 ns with standard deviation of 0.09 ns was measured and the error was 7.4%. The results described above are summarized in Table 1.

To verify the frame rate, ex vivo fluorescence lifetime image of cross section of rabbit artery was recorded in MP4 format (see Video; Supplementary data are available online only). FLIM image was refreshed at a rate of 3.8 frames/sec and video was recorded at 15 frames/sec. Ten micrometer-thick section of the artery sample was stained by 100 μM ICG-DMSO solution over 12-hours. Although the fluorescence lifetime variation (less than 500 ps) in the tissue was observed, the sample preparation procedure was not suitable to elicit any meaningful biological interpretation about such lifetime variation. However, the experiment shows the performance of our system is sufficient to visualize fluorescence lifetime image in various biological tissues on a real-time basis. Snap shots in two field of views are represented in Fig. 12. Lifetimes from 0 to 2 ns were color-mapped by jet colormap from blue to red.

Table 1. Measured lifetimes by TCSPC and AMD

Lifetime	Fluorophore	
	ICG in DMSO (ns)	ICG in methanol (ns)
Nominal (Berezin & Achilefu, 2010)	0.97	0.51
TCSPC	0.97	0.54
AMD	1.05	0.58

TCSPC, time-correlated single photon counting; AMD, analog mean-delay; ICG, indocyanine green; DMSO, dimethyl sulfoxidel.

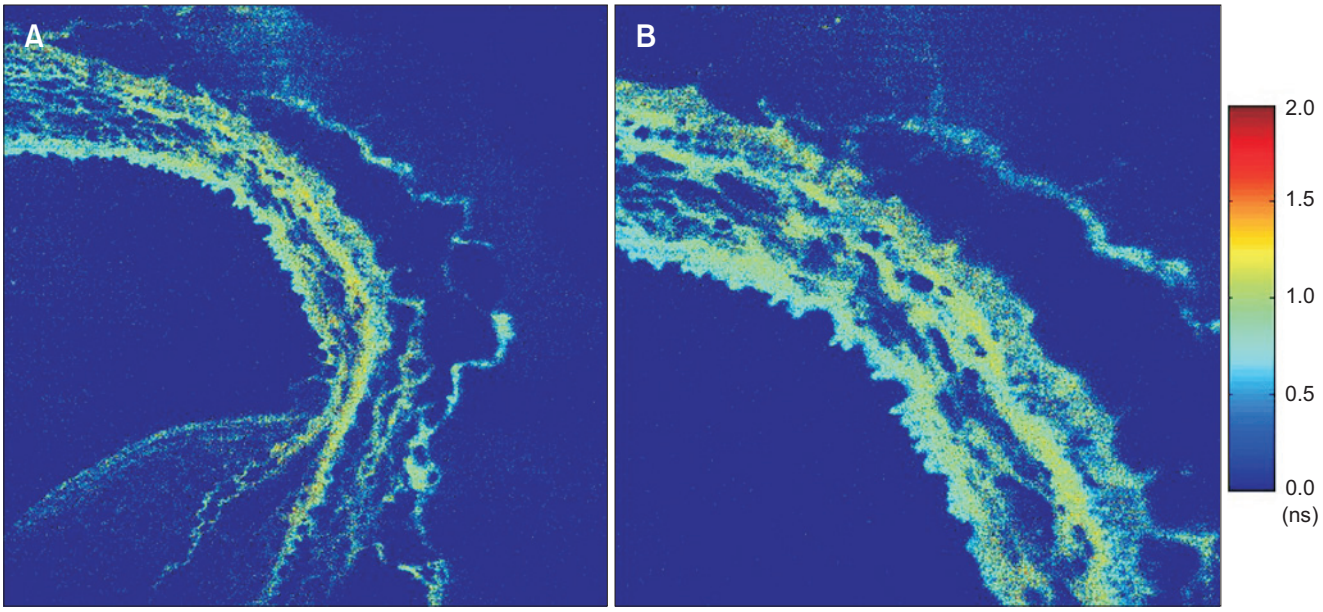

Fig. 12. Snap shots of fluorescence lifetime video of rabbit artery. (A) Field of view (FOV): 600 μm. (B) FOV: 300 μm.

CONCLUSIONS

Real-time FLIM by using AMD method is first implemented in this paper. The most accurate and intriguing TCSPC-FLIM is inherently too slow, and previous AMD-FLIM just saved the acquired data to a storage and frames were reconstructed by post-processing. In this research, however, real-time FLIM was devised and implemented in a true sense of the word and even cost-effectively in comparison to the method using multi-channel TCSPC-FLIM.

Synchronized frames were generated with a rate of 3.8 frames/sec in 1,024×1,024 resolution. This frame rate was limited by the frequency of the resonant scanner, neither by data acquisition nor processing speed. If the slow-axis pixel resolution is decreased to 512 pixels or 256 pixels, the frame rate can be further increased over 7 frames/sec and 15 frame/sec respectively.

In addition, four types of information, a back-scattered confocal reflection image, confocal fluorescence image and their respective lifetime images, can be constructed simultaneously. Unlike previous studies of AMD-FLIM, we measure mean-delay values of IRF and fluorescence simultaneously, so that our system does not need to be calibrated to compensate the effect of trigger time difference.

Although the lifetime measurement error of our AMD-system is under 10% compared to the measurement result using TCSPC, it can be improved according to the photon rate conditions. And the real-time AMD-FLIM has enormous potential in various imaging applications such as three-dimensional imaging, time-lapse tracing of lifetime variation and in vivo imaging. This prospects can be made real by exact frame composition and fast parallel processing of data.

CONFLICT OF INTEREST

No potential conflict of interest relevant to this article was reported.

REFERENCES

Berezin M Y and Achilefu S (2010) Fluorescence lifetime measurements and biological imaging. *Chemical Reviews* **110**, 2641-2684.

Cambridge Technology (2006) *CRS (Counter Rotation Scanner) User's Manual* (Cambridge Technology).

Gilbert D, Franjic-Würtz C, Funk K, Gensch T, Frings S, and Möhrlen F (2007) Differential maturation of chloride homeostasis in primary afferent neurons of the somatosensory system. *Int. J. Devl. Neuroscience* **25**, 479-489.

Hanson K M, Behne M J, Barry N P, Mauro T M, Gratton E, and Clegg R M (2002) Two-photon fluorescence lifetime imaging of the skin stratum corneum pH Gradient. *J. Biophysics* **83**, 1682-1690.

Kim J, Ryu J, and Gweon D (2015) Parametric optimization for high speed FLIM implementation. *MATEC Web of Conference* **32**, 04011.

Köllner M and Wolfrum J (1992) How many photons are necessary for fluorescence-lifetime measurements? *Chem. Phys. Lett.* **200**, 199-204.

Moon S, Won Y, and Kim D Y (2009) Analog mean-delay method for high-speed fluorescence lifetime measurement. *Opt. Express* **17**, 2834-2849.

Park J, Pande P, Shrestha S, Clubb F, Applegate B E, and Jo J A (2012) Biochemical characterization of atherosclerotic plaques by endogenous multispectral fluorescence lifetime imaging microscopy. *Atherosclerosis* **220**, 394-401.

Won Y, Moon S, Yang W, Kim D, Han W T, and Kim D Y (2009) High-speed confocal fluorescence lifetime imaging microscopy (FLIM) with the analog mean delay (AMD) method. *Opt. Express* **19**, 3396-3405.

Won Y J, Moon S, Han W T, and Kim D Y (2010) Referencing techniques for the analog mean-delay method in fluorescence lifetime imaging. *J. Opt. Soc. Am. A* **27**, 2402-2410.